




Understanding the History of Two Complex Ice Crystal Habits Deduced From a Holographic Imager

Journal Article

Author(s):

Pasquier, Julie T.; [Henneberger, Jan](#) ; Korolev, Alexei; Ramelli, Fabiola; [Wieder, Jörg](#) ; Lauber, Annika; Li, Guangyu; David, Robert O.; Carlsen, Tim; Gierens, Rosa; Maturilli, Marion; [Lohmann, Ulrike](#) 

Publication date:

2023-01-16

Permanent link:

<https://doi.org/https://doi.org/10.3929/ethz-b-000593743>

Rights / license:

[Creative Commons Attribution-NonCommercial-NoDerivatives 4.0 International](#)

Originally published in:

Geophysical Research Letters 50(1), <https://doi.org/10.1029/2022GL100247>

Funding acknowledgement:

- LC-CLA-08-2018 | RIA | Constrained aerosol forcing for improved climate projections ()
- Exploiting orographic clouds for constraining the sources of ice crystals ()

Geophysical Research Letters®

RESEARCH LETTER

10.1029/2022GL100247

Key Points:

- A large variety of ice crystal sizes and shapes were observed in Arctic mixed-phase clouds with a holographic imager
- The growth history of two types of complex ice crystals was inferred from their shapes
- These ice crystals could enhance aggregation and secondary ice production

Correspondence to:

J. T. Pasquier and J. Henneberger,
julie.pasquier@env.ethz.ch;
jan.henneberger@env.ethz.ch

Citation:

Pasquier, J. T., Henneberger, J., Korolev, A., Ramelli, F., Wieder, J., Lauber, A., et al. (2023). Understanding the history of two complex ice crystal habits deduced from a holographic imager. *Geophysical Research Letters*, 50, e2022GL100247. <https://doi.org/10.1029/2022GL100247>

Received 12 JUL 2022
 Accepted 18 NOV 2022

Author Contributions:

Conceptualization: J. T. Pasquier, J. Henneberger, U. Lohmann
Data curation: J. T. Pasquier, J. Wieder, G. Li, R. O. David, T. Carlsen, R. Gierens, M. Maturilli
Formal analysis: J. T. Pasquier
Funding acquisition: U. Lohmann
Investigation: J. T. Pasquier, J. Wieder, T. Carlsen, R. Gierens, U. Lohmann
Methodology: J. T. Pasquier, J. Henneberger, A. Korolev, F. Ramelli, A. Lauber, R. O. David, U. Lohmann
Project Administration: J. T. Pasquier, U. Lohmann

© 2023 His Majesty the King in Right of Canada, Institute for atmospheric & climate science, ETH Zurich and The Authors. Reproduced with the permission of the Minister of Environment and Climate Change Canada. This is an open access article under the terms of the [Creative Commons Attribution-NonCommercial-NoDerivs License](https://creativecommons.org/licenses/by/4.0/), which permits use and distribution in any medium, provided the original work is properly cited, the use is non-commercial and no modifications or adaptations are made.

Understanding the History of Two Complex Ice Crystal Habits Deduced From a Holographic Imager

J. T. Pasquier¹ , J. Henneberger¹ , A. Korolev² , F. Ramelli¹, J. Wieder¹, A. Lauber^{1,3} , G. Li¹, R. O. David⁴ , T. Carlsen⁴ , R. Gierens⁵ , M. Maturilli⁶ , and U. Lohmann¹ 

¹Institute for Atmospheric and Climate Science, ETH Zürich, Zurich, Switzerland, ²Environment and Climate Change Canada, Toronto, ON, Canada, ³Now at Center for Climate Systems Modelling (C2SM), ETH Zürich, Zurich, Switzerland, ⁴Department of Geosciences, University of Oslo, Oslo, Norway, ⁵Institute for Geophysics and Meteorology, University of Cologne, Cologne, Germany, ⁶Alfred Wegener Institute, Helmholtz Centre for Polar and Marine Research (AWI), Potsdam, Germany

Abstract The sizes and shapes of ice crystals influence the radiative properties of clouds, as well as precipitation initiation and aerosol scavenging. However, ice crystal growth mechanisms remain only partially characterized. We present the growth processes of two complex ice crystal habits observed in Arctic mixed-phase clouds during the Ny-Ålesund AeroSol Cloud Experiment campaign. First, are capped-columns with multiple columns growing out of the plates' corners that we define as *columns on capped-columns*. These ice crystals originated from cycling through the columnar and plate temperature growth regimes, during their vertical transport by in-cloud circulation. Second, is aged rime on the surface of ice crystals having grown into faceted columns or plates depending on the environmental conditions. Despite their complexity, the shapes of these ice crystals allow to infer their growth history and provide information about the in-cloud conditions. Additionally, these ice crystals exhibit complex shapes and could enhance aggregation and secondary ice production.

Plain Language Summary Snowflakes formed in the atmosphere have a wide variety of shapes and sizes and no two snowflakes are identical. The reason for this infinite number of shapes is that the environmental temperature and relative humidity prevailing during the snowflakes' growth determine their exact aspects. Thus, the prevailing environmental conditions can be determined from the shape of snowflakes, and become more complicated with increased shape complexity. During a measurement campaign in the Arctic, we identified two complex snowflake types and the history of environmental conditions in which they grew in. We inferred that some snowflakes were recirculating to higher or lower parts of the clouds and that others had collided with cloud droplets that froze on their surface at the early stage of their growth. These snowflakes may enhance the formation of new snowflakes and the initiation of precipitation.

1. Introduction

Clouds produce ice crystals of a fascinating diversity of shapes and patterns, and no two single ice crystals are identical (Bentley & Humphreys, 1931). The ice crystal shapes determine their scattering properties (Wyser, 1999) and thus influence the radiative properties of clouds (e.g., Järvinen et al., 2018; Yi et al., 2013). Thus, to reduce the considerable uncertainties related to the cloud's radiative properties (IPCC, 2021), the ice crystal habits need to be correctly described.

Furthermore, the ice crystal sizes and shapes determine their density, and therefore their fall velocities, which impacts their collision rates with other cloud particles. The ice crystal shape influences their interlocking and aggregation efficiencies (Connolly et al., 2012). The collision rate and aggregation efficiency of the ice crystals, in turn, determine precipitation formation. Therefore, an accurate description of the ice crystal habits is important to correctly represent precipitation.

The shape, size, and fall velocity of ice crystals further affect their collision rates with aerosol particles and the scavenging rates, which influence the aerosol concentration and the aerosol radiative forcing (Croft et al., 2009). Thus, to improve the understanding of aerosol scavenging, it is important to understand ice crystal growth mechanisms and to characterize ice crystal habits.

Software: J. Henneberger
Supervision: U. Lohmann
Validation: A. Korolev, A. Lauber
Visualization: J. T. Pasquier
Writing – original draft: J. T. Pasquier
Writing – review & editing: J. T. Pasquier, J. Henneberger, A. Korolev, F. Ramelli, J. Wieder, A. Lauber, G. Li, R. O. David, T. Carlsen, R. Gierens, M. Maturilli, U. Lohmann

The exact shape of ice crystals grown by water vapor diffusion depends on the ambient temperature and water vapor supersaturation with respect to ice (Bailey & Hallett, 2009; Hueholt et al., 2022; Libbrecht, 2005; Nakaya, 1954; Takahashi et al., 1991). If the nucleation energy barrier for the basal face of the ice crystals is lower than that for the prism face, they grow faster toward the basal face and develop into plates (Libbrecht, 2005). In contrast, if the nucleation energy barrier for the prism face is lower than that of the basal face, the growth of the prism face is faster and the ice crystals develop into columns (Libbrecht, 2005). Nakaya (1954) investigated ice crystal shapes of precipitating snowflakes as well as synthetically grown ice crystals and summarized his observations into a so-called *snow crystal morphology diagram*. This diagram shows that the ice crystal's growth is plate-like at temperatures above -3°C , columnar between -3° and -10°C , and plate-like again at colder temperatures. Furthermore, ice crystals exposed to higher supersaturation grow faster and develop into more complicated shapes, such as needles, sheaths, dendrites, and rosettes (Bailey & Hallett, 2009; Knight, 2012; Pruppacher & Klett, 2010), because the supersaturation and hence the crystal growth at tips and edges is faster than at a center of a face (Lamb & Verlinde, 2011). Thus, if ice crystals have a pristine shape, the temperature and supersaturation they experienced during growth by diffusion can be deduced, and the time of formation can be approximated from their size. In other words, the appearance of ice crystals gives information about their history within clouds.

Subsequent to the work of Nakaya (1954), the growth of ice crystal was further studied and the ice crystal morphology diagram improved. For instance (a) Kobayashi (1958) described the growth of ice crystals at low water vapor saturation, (b) Kobayashi (1961), Takahashi et al. (1991) and Fukuta and Takahashi (1999) described the ice crystal growth under free fall in vertical supercooled cloud tunnels, (c) Bailey and Hallett (2004, 2009) improved the ice habit classification for temperatures between -40° and -20°C using laboratory and field measurements, (d) Libbrecht (2005, 2017) described with more precision the physical mechanisms governing the formation of ice crystals and grew ice crystals in controlled conditions in the laboratory. While Nakaya (1954) had already noted the presence of ice particles showing combinations of plate and columnar features in artificially grown ice crystals, Magono and Lee (1966) described in more detail the growth of ice crystals to plates and columns when growing in different environmental conditions and conceived an extensive table including these ice particles. The Magono and Lee (1966) classification has been extensively revised by Kikuchi et al. (2013), who added a group that combines columns and plates.

In addition to growth by diffusion, ice crystals can grow by aggregation with other ice crystals or by riming of cloud droplets on their surface. Ice crystals thereby gradually lose their original shapes, which renders difficult the determination of their history. The majority of the ice crystals in the atmosphere are such irregular ice crystals (e.g., Korolev et al., 1999; Staelin et al., 2007).

Despite the extensive research performed over more than 90 years (e.g., Bentley & Humphreys, 1931; Korolev et al., 1999; Libbrecht, 2017; Nakaya, 1954), the ice crystal growth mechanisms remain only partially understood and characterized (Libbrecht, 2017). This work builds on previous studies investigating the growth history of ice crystals (e.g., Kobayashi, 1961; Libbrecht, 2005; Magono & Lee, 1966; Nakaya, 1954) and extends the analysis to two types of ice particles with complex habits.

2. Methods

The data presented in this paper was collected during the Ny-Ålesund AeroSol Cloud Experiment (NASCENT) campaign, which took place from September 2019 to August 2020 in Ny-Ålesund, Svalbard (78.9°N , 11.9°E), and aimed at enhancing the knowledge about the chemical and microphysical properties of aerosols and clouds in the Arctic climate (Pasquier, David, et al., 2022). In this study, the main instrument used is the HOLOGraphic cloud Imager for Microscopic Objects (HOLIMO) mounted on the tethered balloon system HoloBalloon (Ramelli et al., 2020). HOLIMO uses holography to image cloud particles in the size range from small cloud droplets ($6\ \mu\text{m}$) to large ice particles ($2\ \text{mm}$) in a three-dimensional sample volume of approximately $15\ \text{cm}^3$ (Beck et al., 2017; Henneberger et al., 2013; Ramelli et al., 2020). Particles larger than $25\ \mu\text{m}$ are differentiated between cloud droplets and ice crystals (Henneberger et al., 2013) with the help of a convolutional neural network trained and fine-tuned on cloud particles from holographic imagers (Lauber, 2020; Touloupas et al., 2020). Subsequently, the ice crystals were manually classified according to their shape into the habits: columnar ice crystals including columns and needles, plates, dendrites, frozen drops, and irregular particles that comprise rimed and aggregated ice crystals. Additionally, we describe two complex ice crystal habits in this study.

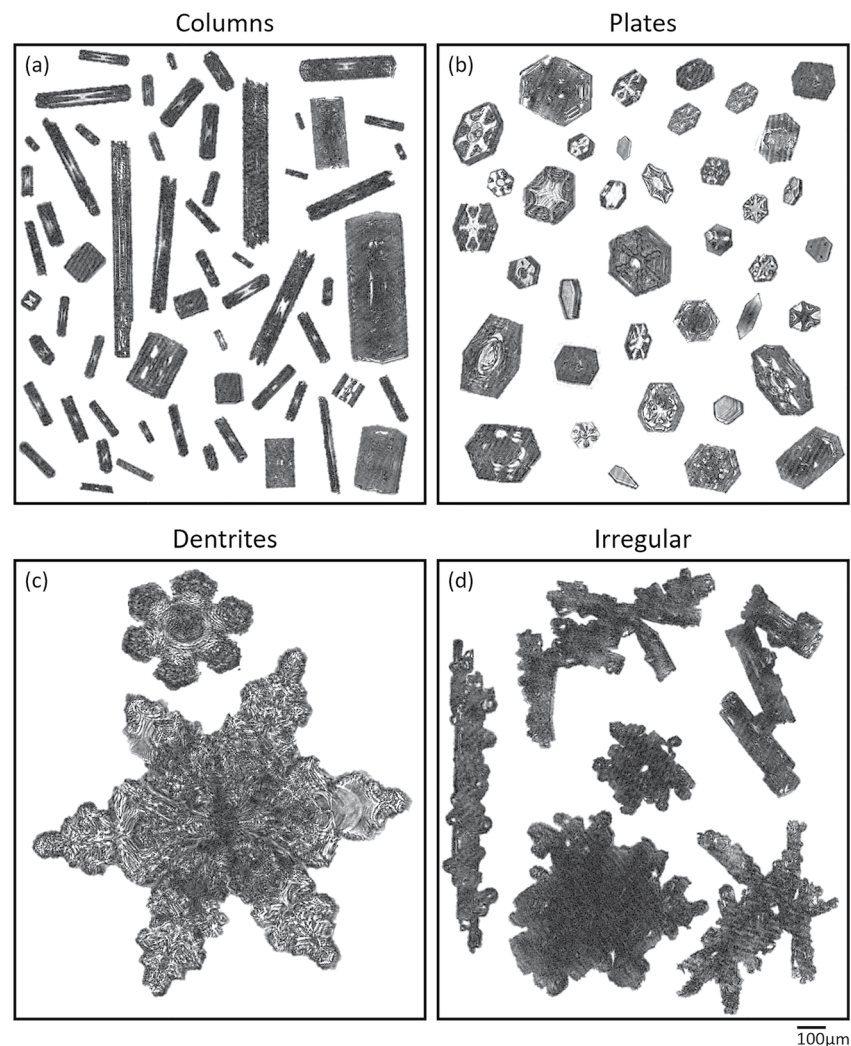


Figure 1. Examples of ice crystals observed with HOLOGraphic cloud Imager for Microscopic Objects and classified manually as (a) columns, (b) plates, (c) dendrites, and (d) irregular ice particles. The scale bar at the bottom right applies for all panels.

The in situ holographic measurements are complemented by ground-based remote sensing instruments installed at the French–German Arctic Research Base AWIPEV. In particular, the 94 GHz cloud radar (JOYRAD-94, Küchler et al., 2017) acquires continuous information on the vertical structure of the clouds. In this study, we use the measured Doppler velocity describing the sum of the updraft and radar reflectivity weighted fall velocities of cloud particles, and the reflectivity, which is proportional to the sizes and concentrations of cloud particles. Daily radiosonde launches (Maturilli & Kayser, 2017) provide information on the vertical distribution of wind, temperature, and humidity in the atmosphere.

3. Results

A large variety of ice crystal sizes and shapes were observed with HOLIMO during the NASCENT campaign. We identified three ice crystal shapes from the morphology diagram (Nakaya, 1954), that is, columnar ice crystals, plates, and dendritic crystals (Figures 1a–1c). The columns had varying lengths (from a few micrometers to ~1 cm) and varying aspect ratios (1–12) (Figure 1a). Hollow columns were identified by their bright centers. The plates ranged in a variety of sizes, thicknesses, and patterns (Figure 1b). The presence of dendritic ice crystals was indicative of high supersaturation with respect to ice in the measured clouds (Figure 1c). In addition to these single faceted ice crystals that we name “pristine” ice crystals, many irregular ice crystals with signs of

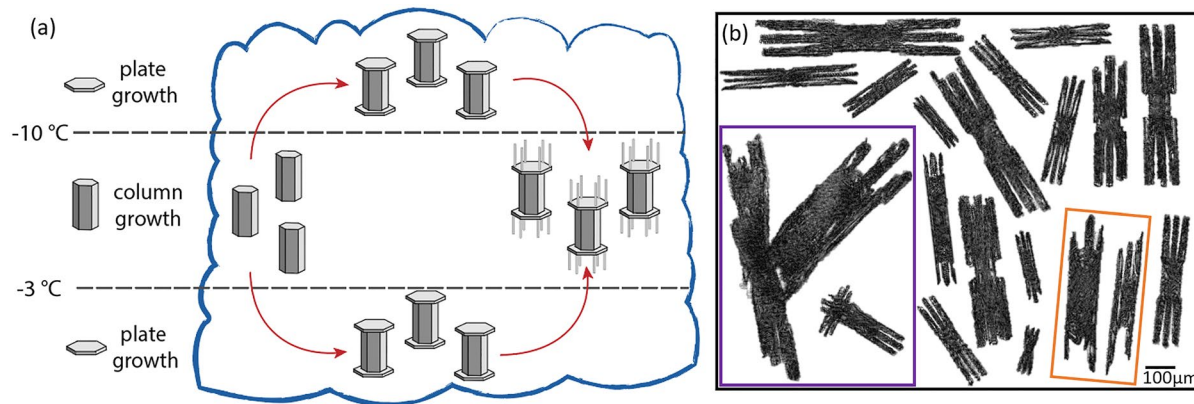


Figure 2. (a) Schematic of the growth of columns on capped-columns (CPC) particles through recirculation within clouds. (b) Examples of CPC particles observed with HOLIMO: two aggregated CPC particles are highlighted with the purple frame, CPC particles with a missing column are highlighted with the orange frame.

aggregation and/or riming were observed (Figure 1d). For these ice crystals, it is impossible to determine with certainty their underlying ice crystal habit(s) (e.g., column, plate, dendrite). Similar ice crystal habits have been reported in other Arctic mixed-phase clouds (e.g., Avramov et al., 2011; Korolev et al., 1999; Lawson et al., 2001; McFarquhar et al., 2007; Mioche et al., 2017; Wendisch et al., 2019; Young et al., 2016). Since these are common habits, they are not discussed further.

We observed two distinguishable complex ice crystal habits for which it was possible to determine their origin and growth history. First, ice particles with combinations of columns and plates were observed. These ice crystals were growing successively in different temperature regimes, which provides evidence for their recirculation within the clouds, and are named *columns on capped-columns* (CPC) here, (Figures 2 and 3). We name them CPC to follow the nomenclature from Kikuchi et al. (2013), who included capped columns in the mixed column/plate category. Second, particles with faceted protuberances originating from growing rime that we define as *aged rime particles* (Figures 4 and 5). The collocation of in situ and remote sensing observations of cloud microphysical variables allows for a detailed look into the growth processes of these two types of ice crystals in the following sections.

3.1. Observations of Columns on Capped-Columns

On 11 November 2019, HoloBalloon collected microphysical measurements in a stratocumulus cloud with cloud droplet number concentration amounting to $1\text{--}5\text{ cm}^{-3}$. A detailed description of the cloud microphysical properties and meteorological conditions on this day is given in Pasquier, Henneberger, Ramelli, Lauber, et al. (2022). The dominant ice crystal habits were columnar and irregular ice crystals (Pasquier, Henneberger, Ramelli, Lauber, et al., 2022). Additionally, capped-columns with multiple columns/needles that grew from the corners of the plates were observed (Figure 2b). Note that these CPC particles have monocrystalline crystallographic lattice. We propose that these CPCs formed by undergoing the following process: ice particles first grew to columns, then plates formed at the basal planes of the column and the ice particles developed into capped-columns, and finally columns grew from the corners of the plates (Figure 2a). This means that the CPCs experienced successive growth in both the columnar ($-3^\circ\text{C} < T < -10^\circ\text{C}$) and plate ($T > -3^\circ\text{C}$ or $T < -10^\circ\text{C}$) temperature regimes. A successive growth in the column—plate—column growth regimes was possible under the prevailing conditions in this cloud as the radiosonde launched at 20:00 UTC measured a temperature of -3°C at 300 m a.s.l., -10°C at 1,300 m a.s.l., and -14°C at cloud top at 2,200 m a.s.l. (Figure 3). Additionally, the Doppler velocity indicated a turbulent cloud structure with rapidly changing updraft/downdraft regions within the cloud, enabling the lifting or falling of cloud particles (Figure 3a). Finally, the high reflectivity ($>0\text{ dBZ}$) reaching up to 1,500 m a.s.l. indicates the presence of larger ice crystals at this altitude (Figure 3b).

We suggest that the CPCs started to grow as columns between -10°C and -3°C at altitudes between 300 m a.s.l. and 1,300 m a.s.l. (Figure 2a). Then, they were transported either upward (above $\sim 1,300\text{ m a.s.l.}$) to colder ($< -10^\circ\text{C}$) or downward (below $\sim 300\text{ m a.s.l.}$) to warmer ($> -3^\circ\text{C}$) regions of the cloud, where plate growth was favored, and developed into capped-columns (Figure 2a). These crystals were then transported back to the

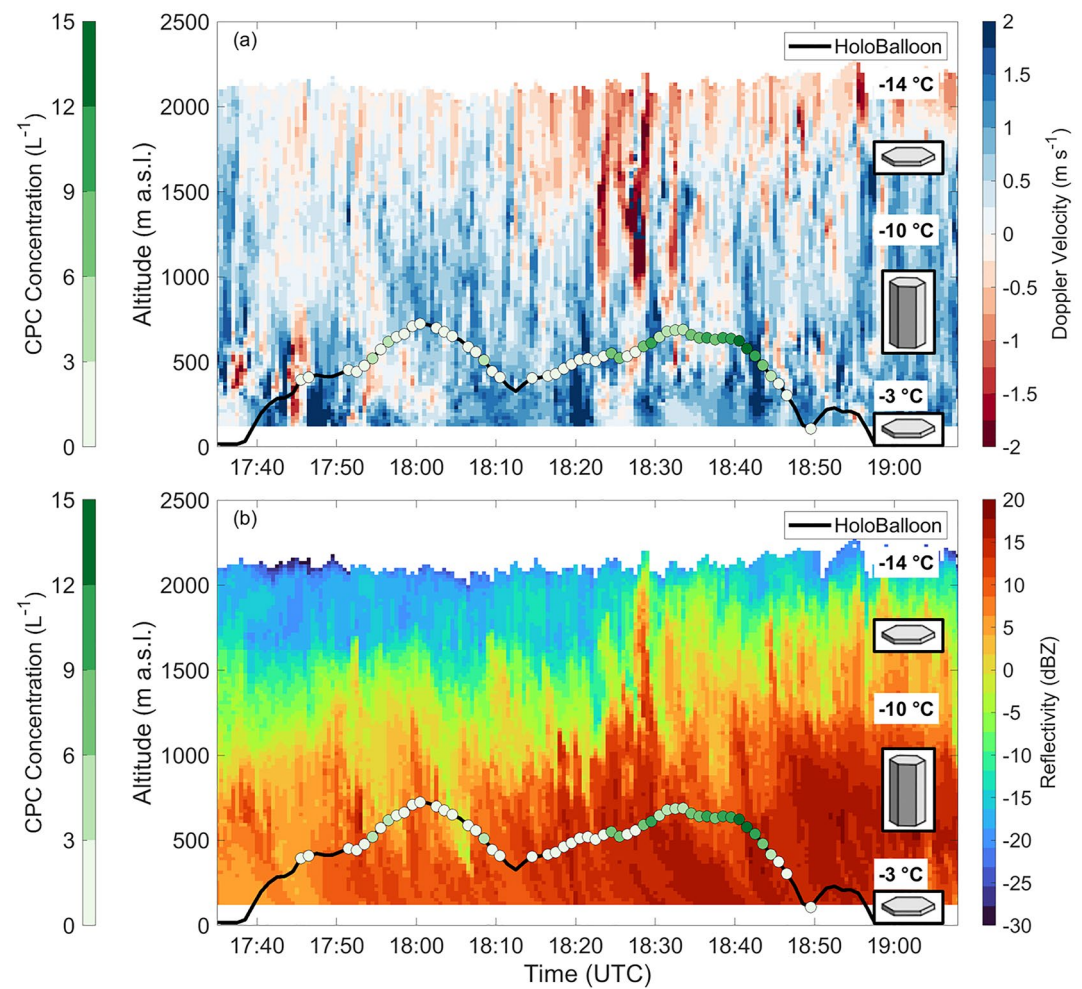


Figure 3. (a) Doppler velocity and (b) reflectivity measured by the cloud radar (color shading). HoloBalloon path (black line), and columns on capped-columns concentration (dots, green shading) measured on 11 November 2019. The indicated temperatures were measured by a radiosonde launched at 20:00 UTC. Plate and column growth regions are illustrated with the respective symbols. Negative Doppler velocities correspond to updrafts in (a).

columnar growth environment, and the columns grew out of the plate corners, where the water vapor supersaturation is highest (Figure 2a). This was the only cloud case during the NASCENT campaign, where CPC particles were measured (likely due to the specific temperature/updraft combination necessary for their formation), but their concentration reached up to 20 L⁻¹ which corresponds to 30% of the total ice crystal number concentration at around 18:40 UTC (Figure 3).

These CPC particles are not listed in the extensive morphology diagram developed by Magono and Lee (1966) and Kikuchi et al. (2013). To our knowledge, similar CPC particles were only observed in natural clouds by Libbrecht (2019) in Fairbanks, Alaska, and by Korolev et al. (2020) during a measurement flight in French Guiana. In both cases, the particles were observed at -5 °C, which corresponds to the temperature range (-4°–-5.5 °C) at which we observed CPC particles on 11 November 2019 in Ny-Ålesund. In addition, we are aware that similar particles could be formed in the laboratory (Libbrecht, 2019), following temperature changes as discussed here.

Several measured CPC particles were aggregated (examples highlighted with purple frame in Figure 2b). It was established that complex dendritic structures favor aggregation by improving mechanical interlocking (Barrett et al., 2019). As the CPC particles exhibit complex structures, they are likewise likely to favor aggregation. Additionally, strong updrafts prevailed, enabling the lifting of ice particles within the cloud. Considerable lifting of ice particles likely increased the residence time of the ice particles in the cloud, allowing them to grow to larger size,

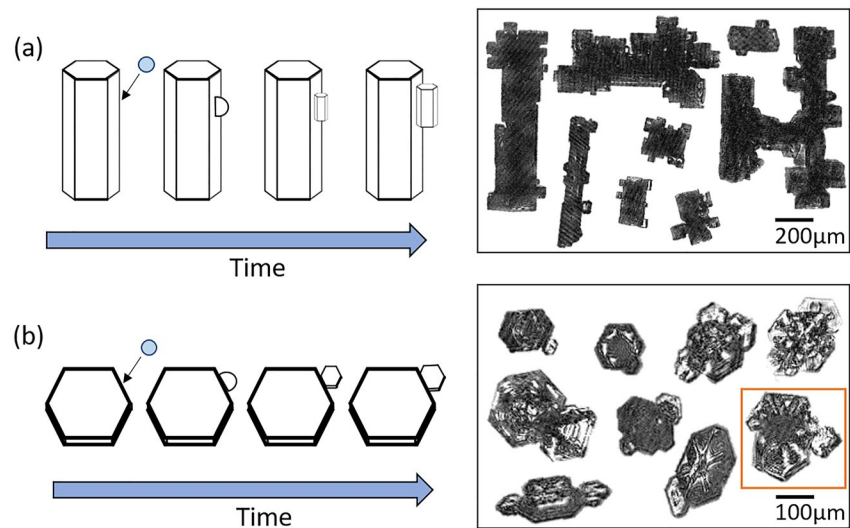


Figure 4. (a) Growth of columns and (b) plates after a cloud droplet collided, rimed, and grew in the columnar or plate regime. These ice crystals are termed aged rime particles, and examples of such ice crystals measured with Holographic cloud Imager for Microscopic Objects are shown in the black frames on the right. An aged rime plate showing signs of breaking up is highlighted with an orange frame.

and increasing the chance of collisions with other particles. The effect of the strong updraft together with complex structures of the CPCs likely favored aggregation and increased precipitation (Chellini et al., 2022).

Some particles were missing one or more columns growing from the plates (see particles highlighted with the orange frame in Figure 2b). As the outer columns of the CPC particles are rather fragile, it is possible that the branches broke off upon collision with other ice crystals or because of strong aerodynamical forces, thereby creating secondary ice crystals. Indeed, secondary ice production was found to be enhanced between 18:20 UTC and 18:45 UTC on 11 November 2019, as described in Pasquier, Henneberger, Ramelli, Lauber, et al. (2022).

3.2. Observations of Aged Rime Particles

Other ice crystals observed during the flight on 11 November 2019 with HOLIMO were aged rime columns. These particles have particular faceted protuberances that grew in the columnar growth regime, similar to the original column (Figure 4a). Ice crystals showing similar, but plate-like, faceted protuberances growing on plates were observed on 1 April 2020 (Figure 4b). On this day, the temperature in the cloud measured with HoloBalloon varied between -23.5° and -15°C (Figure 5), hence in the plate growth regime at low supersaturation with respect to ice (Nakaya, 1954). The increase in the radar reflectivity between 2,000 and 1,000 m indicates that the layer was saturated with respect to ice. Moreover, the sharp increase in the radar reflectivity between 1,200 and 1,000 m suggests the presence of an embedded supercooled liquid layer (Figure 5b), which is supported by the increase in cloud droplet number concentrations up to 10 cm^{-3} in some regions as described in Pasquier, Henneberger, Ramelli, Lauber, et al. (2022). Aggregation may have contributed to the increase in reflectivity. Doppler velocities showed few variations except at around 14:30 UTC (Figure 5a). We propose that the formation of aged rime ice crystals occurs as follows (Figure 4): first cloud droplets rime on the columnar or plate-like ice crystal and freeze. The frozen protuberances then grow on the basal face (plate growth regime) or prism face (columnar growth regime) depending on the temperature and supersaturation experienced. Note that the orientation of the growing protuberance in the basal or prism face remains identical to that of the original ice crystal (Iwabuchi & Magono, 1975; Pitter & Pruppacher, 1973; Uyeda & Kikuchi, 1978). Thus, these crystals are faceted single crystal ice particles. This creates faceted protuberances observed on aged rime particles, compared to the smaller round protuberances observed on freshly rimed ice crystals. The presence of aged rime ice without fresh rime suggests that the ice crystal originates from a region with a higher liquid water content and spent some time in the ice supersaturated, but liquid water subsaturated environment, sufficient to develop facets on the frozen droplets. As aged rime ice crystal concentrations up to 25 L^{-1} were measured during the HoloBalloon flight,

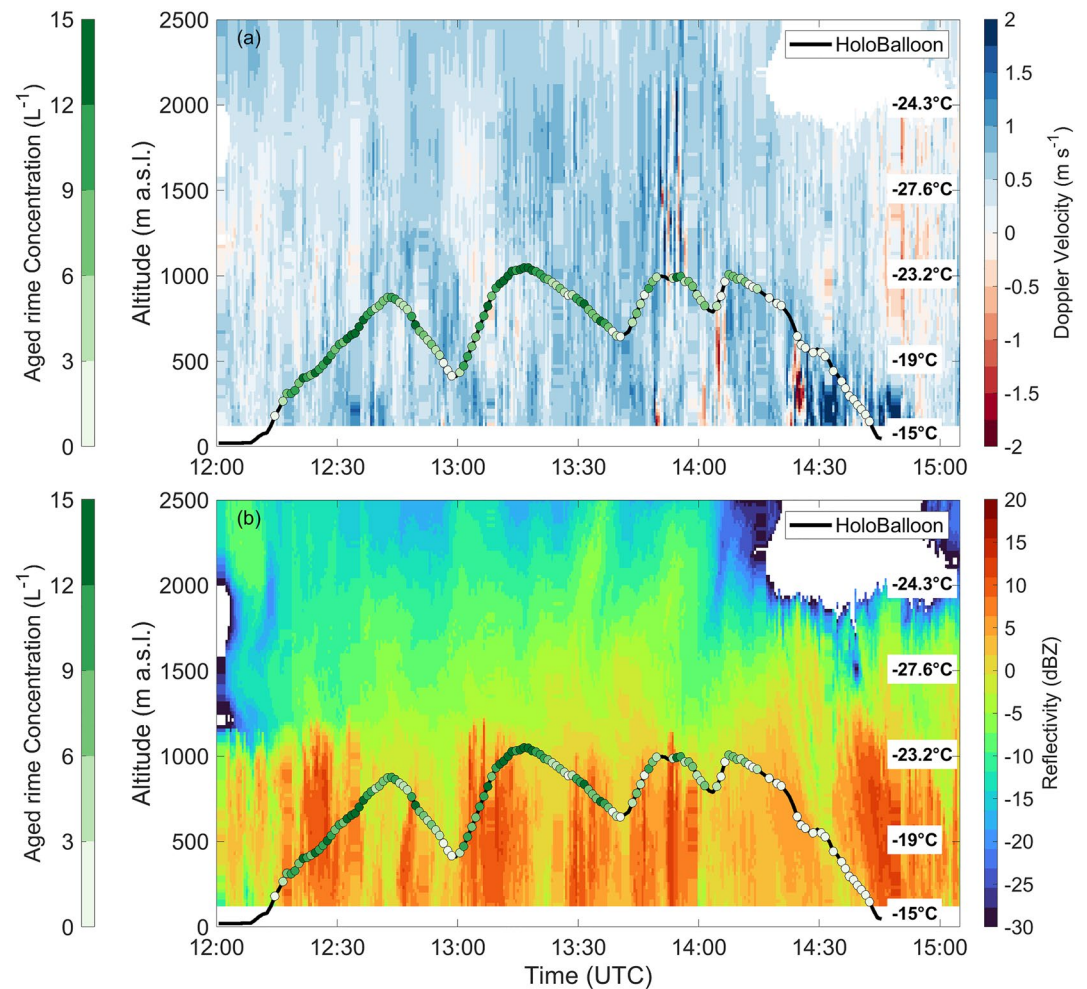


Figure 5. (a) Doppler velocity and (b) reflectivity measured by the cloud radar (color shading). HoloBalloon path (black line), and columns on capped-columns concentration (dots, green shading) measured on 1 April 2020. The temperature is indicated every 500 m in altitude as measured by the radiosonde launched at 17:00 UTC.

we propose that the aged rime ice crystal experienced riming in the embedded supercooled liquid layer between 1,000 and 1,200 m a.s.l. and grew to aged rime ice crystals during sedimentation to the altitude of HoloBalloon.

The presence of rime growing to faceted protuberances was already mentioned by Libbrecht (2005) for laboratory grown ice crystals and by Korolev et al. (2020) in natural clouds. Recently, Waitz et al. (2022) investigated riming in Arctic mixed-phase clouds and described similar aged rime particles as “epitaxially” rimed in contrast to “normal” rimed ice particles, the former most frequently prevailing in the temperature range between -10° and 0°C . It is interesting to note that aged rime ice crystals could be mistaken for aggregated particles due to their similar shapes. However, their formation arises from riming and not from aggregation.

Several aged rime plates showed evidence of breaking up, as the particle highlighted with the orange frame in Figure 4b. The fragility of the aged rime plate particles could augment their chance of breaking up upon collision with other ice crystals. Therefore they could favor secondary ice production via the ice-ice collision process, as discussed in Pasquier, Henneberger, Ramelli, Lauber, et al. (2022).

4. Summary

The habits of pristine ice crystals can be used to identify their growth history within clouds, but determining the history of complex ice crystals that experienced aggregation or riming is difficult. Here, we present two types of complex ice crystal habits observed in Arctic mixed-phase clouds during the NASCENT campaign, revealing their growth history despite their complex shapes.

First, the CPC particles were growing successively in the column and plate growth regimes and exhibited a unique ice crystal shape corresponding to a capped-column with columns growing out of the corner of their plates (Figure 2). Because the plate and column growth regimes are temperature constrained, we could determine that these ice crystals were recirculating between the upper and/or lower parts of the clouds where the temperature was below -10°C or above -3°C (plate growth regimes), and the column growth regime between -10° and -3°C .

Second, aged rime plates and columns exhibiting faceted protuberances were observed, indicative of rime at the earlier stages of their growth process. After the rime froze on the surface of the plates and columns, it grew as a faceted protuberance with the same habit and along the same axis as the original ice crystal.

The observed CPC particles and aged rime ice crystals likely influence the cloud properties. CPC particles possibly favor aggregation by facilitating mechanical interlocking similarly to dendritical ice crystals (Barrett et al., 2019; Chellini et al., 2022), thereby enhancing precipitation and scavenging. For instance, on 11 November 2019, the precipitation rate was highest between 18:00 and 19:00 UTC, when the concentration of CPC particles was the highest (not shown). The high surface to volume ratio of the aged rime plates might enhance aerosol scavenging, thereby influencing the aerosol-cloud interactions. Furthermore, observations of broken ice crystals suggest that both the outer columns of the CPC particles and the protuberances of the aged rime plates are fragile and thus could easily break off upon collision (Pasquier, Henneberger, Ramelli, Lauber, et al., 2022; Takahashi et al., 1995). Therefore, these ice crystals might favor secondary ice production via the ice-ice collision process. More work should be performed to determine the impact of these two complex types of ice crystals on the cloud radiative properties.

Data Availability Statement

The HOLIMO data set and cloud radar data are available for download at: <https://doi.org/10.5281/zenodo.7402285> (Pasquier, Henneberger, Ramelli, Wieder, et al., 2022). The scripts to reproduce the figures are available at: <https://doi.org/10.5281/zenodo.7402296> (Pasquier, Henneberger, & Ramelli, 2022). The radiosonde data are available for download on PANGAEA: <https://doi.org/10.1594/PANGAEA.911039> (Maturilli, 2020a) & <https://doi.org/10.1594/PANGAEA.917967> (Maturilli, 2020b).

References

- Avramov, A., Ackerman, A. S., Fridlind, A. M., van Diedenhoven, B., Botta, G., Aydin, K., et al. (2011). Toward ice formation closure in arctic mixed-phase boundary layer clouds during ISDAC. *Journal of Geophysical Research*, 116(D1), D00T08. <https://doi.org/10.1029/2011JD015910>
- Bailey, M., & Hallett, J. (2004). Growth rates and habits of ice crystals between -20° and -70°C . *Journal of the Atmospheric Sciences*, 61(5), 514–544. [https://doi.org/10.1175/1520-0469\(2004\)061<0514:GRAHOI>2.0.CO;2](https://doi.org/10.1175/1520-0469(2004)061<0514:GRAHOI>2.0.CO;2)
- Bailey, M., & Hallett, J. (2009). A comprehensive habit diagram for atmospheric ice crystals: Confirmation from the laboratory, air, and other field studies. *Journal of the Atmospheric Sciences*, 66(9), 2888–2899. <https://doi.org/10.1175/2009JAS2883.1>
- Barrett, A. I., Westbrook, C. D., Nicol, J. C., & Stein, T. H. M. (2019). Rapid ice aggregation process revealed through triple-wavelength Doppler spectrum radar analysis. *Atmospheric Chemistry and Physics*, 19(8), 5753–5769. <https://doi.org/10.5194/acp-19-5753-2019>
- Beck, A., Henneberger, J., Schöpfer, S., Fugal, J., & Lohmann, U. (2017). Hologondel: In situ cloud observations on a cable car in the Swiss Alps using a holographic imager. *Atmospheric Measurement Techniques*, 10(2), 459–476. <https://doi.org/10.5194/amt-10-459-2017>
- Bentley, W. A., & Humphreys, W. J. (1931). *Snow crystals* (p. 226). McGraw-Hill Book Company, Inc.
- Chellini, G., Gierens, R., & Kneifel, S. (2022). Ice aggregation in arctic shallow mixed-phase clouds: Enhanced by dendritic growth and absent close to the melting level. *Earth and Space Science Open Archive*, 32. <https://doi.org/10.1002/essoar.10511005.1>
- Connolly, P. J., Emersic, C., & Field, P. R. (2012). A laboratory investigation into the aggregation efficiency of small ice crystals. *Atmospheric Chemistry and Physics*, 12(4), 2055–2076. <https://doi.org/10.5194/acp-12-2055-2012>
- Croft, B., Lohmann, U., Martin, R. V., Stier, P., Wurzel, S., Feichter, J., et al. (2009). Aerosol size-dependent below-cloud scavenging by rain and snow in the ECHAM5-HAM. *Atmospheric Chemistry and Physics*, 9(14), 4653–4675. <https://doi.org/10.5194/acp-9-4653-2009>
- Fukuta, N., & Takahashi, T. (1999). The growth of atmospheric ice crystals: A summary of findings in vertical supercooled cloud tunnel studies. *Journal of the Atmospheric Sciences*, 56(12), 1963–1979. [https://doi.org/10.1175/1520-0469\(1999\)056<1963:TGOAIC>2.0.CO;2](https://doi.org/10.1175/1520-0469(1999)056<1963:TGOAIC>2.0.CO;2)
- Henneberger, J., Fugal, J. P., Stetzer, O., & Lohmann, U. (2013). HOLIMO II: A digital holographic instrument for ground-based in situ observations of microphysical properties of mixed-phase clouds. *Atmospheric Measurement Techniques*, 6(11), 2975–2987. <https://doi.org/10.5194/amt-6-2975-2013>

Acknowledgments

This project has received funding from the European Union's Horizon 2020 research and innovation programme under Grant agreement No 821205 (FORCeS), from the Swiss Polar Institute (Exploratory Grants 2018), and from the Swiss National Science Foundation (SNSF) (Grant 200021_175824). We gratefully acknowledge the funding by the European Research Council (ERC) through Grant StG758005. We acknowledge EEARO-NO-2019-0423/IceSafari, contract no. 31/2020, under the NO Grants 2014–2021 of EEA Grants/Norway Grants for financial support. We gratefully acknowledge the funding by the Deutsche Forschungsgemeinschaft (DFG, German Research Foundation)—Project-ID 268020496—TRR 172, within the Transregional Collaborative Research Center “Arctic Amplification: Climate Relevant Atmospheric and Surface Processes, and Feedback Mechanisms (AC)³.” We thank Roland Neuber and Paul Zieger for their support during the organization of the campaigns. The authors thank all those involved in the field work associated with NASCENT. Finally, we thank the reviewers for their constructive and helpful feedback on the manuscript, which strengthened the paper.

- Hueholt, D. M., Yuter, S. E., & Miller, M. A. (2022). Revisiting diagrams of ice growth environments. *Bulletin of the American Meteorological Society*, 103(11), E2584–E2603. <https://doi.org/10.1175/BAMS-D-21-0271.1>
- IPCC. (2021). *Climate change 2021: The physical science basis. Contribution of working group I to the sixth assessment report of the intergovernmental panel on climate change*. In V. Masson-Delmotte, P. Zhai, A. Pirani, S.L. Connors, C. Péan, S. Berger, et al. (Eds.), Cambridge University Press. in press.
- Iwabuchi, T., & Magono, C. (1975). A laboratory experiment on the freezing electrification of freely falling water droplets. *Journal of the Meteorological Society of Japan. Series II*, 53(6), 393–401. https://doi.org/10.2151/jmsj1965.53.6_393
- Järvinen, E., Jourdan, O., Neubauer, D., Yao, B., Liu, C., Andreae, M. O., et al. (2018). Additional global climate cooling by clouds due to ice crystal complexity. *Atmospheric Chemistry and Physics*, 18(21), 15767–15781. <https://doi.org/10.5194/acp-18-15767-2018>
- Kikuchi, K., Kameda, T., Higuchi, K., & Yamashita, A. (2013). A global classification of snow crystals, ice crystals, and solid precipitation based on observations from middle latitudes to Polar Regions. *Atmospheric Research*, 132–133, 460–472. <https://doi.org/10.1016/j.atmosres.2013.06.006>
- Knight, C. A. (2012). Ice growth from the vapor at -5°C . *Journal of the Atmospheric Sciences*, 69(6), 2031–2040. <https://doi.org/10.1175/JAS-D-11-0287.1>
- Kobayashi, T. (1958). On the habit of snow crystals artificially produced at low pressures. *Journal of the Meteorological Society of Japan. Series II*, 36(5), 193–208. https://doi.org/10.2151/jmsj1923.36.5_193
- Kobayashi, T. (1961). The growth of snow crystals at low supersaturations. *The Philosophical Magazine: A Journal of Theoretical Experimental and Applied Physics*, 6(71), 1363–1370. <https://doi.org/10.1080/14786436108241231>
- Korolev, A., Heckman, I., Wolde, M., Ackerman, A. S., Fridlind, A. M., Ladino, L. A., et al. (2020). A new look at the environmental conditions favorable to secondary ice production. *Atmospheric Chemistry and Physics*, 20(3), 1391–1429. <https://doi.org/10.5194/acp-20-1391-2020>
- Korolev, A., Isaac, G. A., & Hallett, J. (1999). Ice particle habits in arctic clouds. *Geophysical Research Letters*, 26(9), 1299–1302. <https://doi.org/10.1029/1999GL900232>
- Küchler, N., Kneifel, S., Löhnert, U., Kollias, P., Czekala, H., & Rose, T. (2017). A W-band radar-radiometer system for accurate and continuous monitoring of clouds and precipitation. *Journal of Atmospheric and Oceanic Technology*, 34(11), 2375–2392. <https://doi.org/10.1175/JTECH-D-17-0019.1>
- Lamb, D., & Verlinde, J. (2011). *Physics and chemistry of clouds*. Cambridge University Press.
- Lauber, A. (2020). *In situ observations of ice multiplication in clouds using a holographic imager and a deep learning algorithm for the classification of cloud particles*. Doctoral dissertation, ETH Zurich. <https://doi.org/10.3929/ethz-b-000474830>
- Lawson, R. P., Baker, B. A., Schmitt, C. G., & Jensen, T. L. (2001). An overview of microphysical properties of Arctic clouds observed in May and July 1998 during FIRE ACE. *Journal of Geophysical Research*, 106(D14), 14989–15014. <https://doi.org/10.1029/2000JD900789>
- Libbrecht, K. G. (2005). The physics of snow crystals. *Reports on Progress in Physics*, 68(4), 855–895. <https://doi.org/10.1088/0034-4885/68/4/r03>
- Libbrecht, K. G. (2017). Physical dynamics of ice crystal growth. *Annual Review of Materials Research*, 47(1), 271–295. <https://doi.org/10.1146/annurev-matsci-070616-124135>
- Libbrecht, K. G. (2019). Snow crystals. arXiv. Retrieved from <https://arxiv.org/abs/1910.06389>
- Magono, C., & Lee, C. W. (1966). Meteorological classification of natural snow crystals. *Journal of the Faculty of Science, Hokkaido University—Series 7: Geophysics*, 2(4), 321–335.
- Maturilli, M. (2020a). High resolution radiosonde measurements from station Ny-Ålesund (2019–11) [Dataset]. Alfred Wegener Institute – Research Unit Potsdam, PANGAEA. <https://doi.org/10.1594/PANGAEA.911039>
- Maturilli, M. (2020b). High resolution radiosonde measurements from station Ny-Ålesund (2020–04) [Dataset]. Alfred Wegener Institute – Research Unit Potsdam, PANGAEA. <https://doi.org/10.1594/PANGAEA.917967>
- Maturilli, M., & Kayser, K. (2017). Arctic warming, moisture increase and circulation changes observed in the Ny-Ålesund homogenized radiosonde record. *Theoretical and Applied Climatology*, 130(1–17), 1434–4483. <https://doi.org/10.1007/s00704-016-1864-0>
- McFarquhar, G. M., Zhang, G., Poellot, M. R., Kok, G. L., McCoy, R., Tooman, T., et al. (2007). Ice properties of single-layer stratocumulus during the mixed-phase arctic cloud experiment: 1. Observations. *Journal of Geophysical Research*, 112(D24), D24201. <https://doi.org/10.1029/2007JD008633>
- Mioche, G., Jourdan, O., Delanoë, J., Gourbeyre, C., Febvre, G., Dupuy, R., et al. (2017). Vertical distribution of microphysical properties of arctic springtime low-level mixed-phase clouds over the Greenland and Norwegian seas. *Atmospheric Chemistry and Physics*, 17(20), 12845–12869. <https://doi.org/10.5194/acp-17-12845-2017>
- Nakaya, U. (1954). *Snow crystals: Natural and artificial*. Harvard University Press.
- Pasquier, J. T., David, R. O., Freitas, G., Gierens, R., Gramlich, Y., Haslett, S., et al. (2022). *The Ny-Ålesund aerosol cloud experiment (nascent): Overview and first results*. Bulletin of the American Meteorological Society. Retrieved from <https://journals.ametsoc.org/view/journals/bams/aop/BAMS-D-21-0034.1/BAMS-D-21-0034.1.xml>
- Pasquier, J. T., Henneberger, J., & Ramelli, F. (2022). Scripts for the publication "Understanding the history of two complex ice crystal habits deduced from a holographic imager". Zenodo. <https://doi.org/10.5281/zenodo.7402296>
- Pasquier, J. T., Henneberger, J., Ramelli, F., Lauber, A., David, R. O., Wieder, J., et al. (2022). Conditions favorable for secondary ice production in arctic mixed-phase clouds. *Atmospheric Chemistry and Physics Discussions*, 1–33. <https://doi.org/10.5194/acp-2022-314>
- Pasquier, J. T., Henneberger, J., Ramelli, F., Wieder, J., Gierens, R., Ebell, K., et al. (2022). Data from the NASCENT campaign used in the publications: "Conditions favorable for secondary ice production in Arctic mixed-phase clouds" and "Understanding the history of two complex ice crystal habits deduced from a holographic imager" [Dataset]. Zenodo. <https://doi.org/10.5281/zenodo.7402285>
- Pitter, R. L., & Pruppacher, H. R. (1973). A wind tunnel investigation of freezing of small water drops falling at terminal velocity in air. *Quarterly Journal of the Royal Meteorological Society*, 99(421), 540–550. <https://doi.org/10.1002/qj.49709942111>
- Pruppacher, H., & Klett, J. (2010). Microphysics of clouds and precipitation. In *Microphysics of clouds and precipitation*. Springer. <https://doi.org/10.1007/978-0-306-48100-0>
- Ramelli, F., Beck, A., Henneberger, J., & Lohmann, U. (2020). Using a holographic imager on a tethered balloon system for microphysical observations of boundary layer clouds. *Atmospheric Measurement Techniques*, 13(2), 925–939. <https://doi.org/10.5194/amt-13-925-2020>
- Stoelinga, M. T., Locatelli, J. D., & Woods, C. P. (2007). The occurrence of "irregular" ice particles in stratiform clouds. *Journal of the Atmospheric Sciences*, 64(7), 2740–2750. <https://doi.org/10.1175/JAS3962.1>
- Takahashi, T., Endoh, T., Wakahama, G., & Fukuta, N. (1991). Vapor diffusional growth of free-falling snow crystals between -3 and -23°C . *Journal of the Meteorological Society of Japan. Series II*, 69(1), 15–30. https://doi.org/10.2151/jmsj1965.69.1_15
- Takahashi, T., Nagao, Y., & Kushiyama, Y. (1995). Possible high ice particle production during graupel–graupel collisions. *Journal of the Atmospheric Sciences*, 52(24), 4523–4527. [https://doi.org/10.1175/1520-0469\(1995\)052<4523:PHIPPD>2.0.CO;2](https://doi.org/10.1175/1520-0469(1995)052<4523:PHIPPD>2.0.CO;2)

- Touloupas, G., Lauber, A., Henneberger, J., Beck, A., & Lucchi, A. (2020). A convolutional neural network for classifying cloud particles recorded by imaging probes. *Atmospheric Measurement Techniques*, *13*(5), 2219–2239. <https://doi.org/10.5194/amt-13-2219-2020>
- Uyeda, H., & Kikuchi, K. (1978). Freezing experiment of supercooled water droplets frozen by using single crystal ice. *Journal of the Meteorological Society of Japan. Series II*, *56*(1), 43–51. https://doi.org/10.2151/jmsj1965.56.1_43
- Wäitz, F., Schnaiter, M., Leisner, T., & Järvinen, E. (2022). In situ observation of riming in mixed-phase clouds using the PHIPS probe. *Atmospheric Chemistry and Physics*, *22*(11), 7087–7103. <https://doi.org/10.5194/acp-22-7087-2022>
- Wendisch, M., Macke, A., Ehrlich, A., Lüpkes, C., Mech, M., Chechin, D., et al. (2019). The Arctic cloud puzzle: Using ALOUD/PASCAL multiplatform observations to unravel the role of clouds and aerosol particles in Arctic amplification. *Bulletin of the American Meteorological Society*, *100*(5), 841–871. <https://doi.org/10.1175/BAMS-D-18-0072.1>
- Wyser, K. (1999). Ice crystal habits and solar radiation. *Tellus A: Dynamic Meteorology and Oceanography*, *51*(5), 937–950. <https://doi.org/10.3402/tellusa.v51i5.14503>
- Yi, B., Yang, P., Baum, B. A., L'Ecuyer, T., Oreopoulos, L., Mlawer, E. J., et al. (2013). Influence of ice particle surface roughening on the global cloud radiative effect. *Journal of the Atmospheric Sciences*, *70*(9), 2794–2807. <https://doi.org/10.1175/JAS-D-13-020.1>
- Young, G., Jones, H. M., Choulaton, T. W., Crosier, J., Bower, K. N., Gallagher, M. W., et al. (2016). Observed microphysical changes in Arctic mixed-phase clouds when transitioning from sea ice to open ocean. *Atmospheric Chemistry and Physics*, *16*(21), 13945–13967. <https://doi.org/10.5194/acp-16-13945-2016>